

Expression and regulation of carbonic anhydrases in the marine diatom *Thalassiosira pseudonana* and in natural phytoplankton assemblages from Great Bay, New Jersey

Patrick J. McGinn* and François M. M. Morel

Department of Geosciences, Guyot Hall, Princeton University, Princeton, NJ 08544, USA

Correspondence

*Corresponding author,
e-mail: pmcginn@princeton.edu

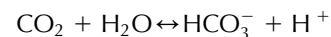
Received 3 October 2007; revised 19
November 2007

doi: 10.1111/j.1399-3054.2007.01039.x

BLAST searches of expressed sequence tag libraries have revealed putative homologs of the archetypal diatom δ -carbonic anhydrase (CA) TWCA1 (for *Thalassiosira weissflogii* CA) in a broad range of eukaryotic phytoplankton including haptophytes, prasinophytes and dinoflagellates. Four putative homologs of TWCA1 are also reported and described from a search of the genomic sequence of *Thalassiosira pseudonana* and designated TWCA_{TP1–4}. The δ -CA class is therefore more widely distributed in marine phytoplankton than previously thought. In particular, it is not restricted to the diatoms like the cadmium-containing enzyme, CDCA, seems to be (ζ -CA class). Zinc status strongly influences growth rate in marine diatoms. We observed a decrease in the specific growth rate of *T. pseudonana* from 2.1 to 1.3 day⁻¹ when the unchelated Zn concentration (Zn') was lowered from 20 to 5 pM. In the same cultures, we detected a drop in whole-cell CA activity of about 50% in the most Zn-limited cells that occurred simultaneously with a large downregulation of TWCA_{TP1}, TWCA_{TP2} and CDCA_{TP} gene transcripts and protein. These three genes were also found to be strongly upregulated by low pCO₂ in a manner typical of many algal CA enzymes. We have also conducted field experiments in diatom-dominated natural phytoplankton assemblages sampled from Great Bay of the coast of New Jersey. We observed increased total CA activity in parallel with increased expression of homologous *twca* and *cdca* gene transcripts in water incubated at increasingly higher pH values. Immunoblot and transcript expression analyses demonstrated a clear upregulation of CDCA transcript and protein as incubation pH increased both in the lab and in the field indicating that this CA is expressed under a broad range of environmental conditions and not restricted to low pCO₂ and low Zn.

Introduction

Carbonic anhydrases (CAs, EC 4.2.1.1) are a large and diverse collection of Zn metalloenzymes that catalyze the equilibration of dissolved inorganic carbon species according to the following equation:



The essential nature of this reaction in diverse biological systems has driven the evolution of several distinct and unrelated families of CAs (Hewett-Emmett and Tashian 1996). Animals possess α -CAs that are

Abbreviations – CA, carbonic anhydrase; CDCA1, cadmium-containing ζ -class CA isolated from *Thalassiosira weissflogii*; *cdca*_{TP}/*CDCA*_{TP}, homologous *cdca* gene/protein in *T. pseudonana*; EST, expressed sequence tag; pCO₂, partial pressure of CO₂; TWCA1 –27 kDa, Zn(Co)-dependent δ -class CA isolated from *T. weissflogii*; *twca*_{TP}/*TWCA*_{TP}, homologous *twca* gene/protein in *T. pseudonana*.

perhaps the best studied family. In this diverse group, the Zn metal center is coordinated by the imidazole rings of three histidine residues. Green plants and cyanobacteria contain β -CAs that also use Zn in the active site but are differentiated from α -CAs by virtue of the fact that the active site is coordinated by a pair of cysteine residues and a single histidine residue.

CAs play a key role in photosynthetic CO₂ assimilation in marine phytoplankton, especially under low-CO₂ conditions (Badger 2003). Carbon dioxide can potentially limit phytoplankton growth owing to the combined effects of a low bioavailability of CO₂ in seawater and the low biochemical affinity for CO₂ displayed by virtually all forms of algal RubisCO (Badger et al. 1998, Tortell 2000). In terms of their role in CO₂ acquisition, CAs targeted to the extracellular space of phytoplankton prevent CO₂ limitation by ensuring a high rate of CO₂ supply to the cell by catalyzing the otherwise slow conversion of HCO₃⁻ to CO₂, which is readily taken up. The conventional role of intracellular CA has been to ensure a high rate of CO₂ supply to RubisCO by rapid dehydration of the HCO₃⁻ pool accumulated in the chloroplast (Kaplan and Reinhold 1999). In marine diatoms, however, efforts to detect chloroplastic CA with fluorescently labeled antibodies in the diatom *Thalassiosira weissflogii* were not successful (Morel et al. 2002). The apparent absence of CA in the chloroplast of this diatom is presumably related to the occurrence of a C4 pathway for C fixation, whereby CO₂ is supplied to RubisCO through catalyzed decarboxylation of oxaloacetate formed by fixation of HCO₃⁻ to phosphoenolpyruvate by phosphoenolpyruvate carboxylase (PEPCase; McGinn and Morel 2008, Reinfelder et al. 2000, 2004, Roberts et al. 2007). In this scenario, chloroplastic CA has the potential to dissipate the CO₂ pool before fixation by RubisCO by converting it back to HCO₃⁻ and so would have a deleterious effect. It is worth mentioning, however, that some diatoms that exhibit characteristics of C4 photosynthesis have also been shown to contain chloroplastic forms of CA (McGinn and Morel 2008, Satoh et al. 2001). Thus, the exact role of chloroplastic CAs in diatoms, if present, remains an unresolved issue. Intracellular CA in diatoms could function to supply HCO₃⁻ to cytoplasmically localized PEPCase by hydrating CO₂ diffusing into the cell or out of the chloroplast (Hatch and Burnell 1990).

In recent years, much has been learned concerning the different forms of CAs occurring in marine phytoplankton and their regulation by environmental factors such as pCO₂ and trace metal status (Lane and Morel 2000a, 2000b, Lee and Morel 1995, Morel et al. 2002, Sunda and Huntsman 1995, Yee and Morel 1996). A 27-kDa CA, named TWCA1, has been isolated from the centric diatom *T. weissflogii* and is regulated by the typical

environmental modulators of CAs, namely pCO₂ and Zn concentrations (Roberts et al. 1997). TWCA1 was the first such CA isolated from a diatom and, as it showed no homology to any known CA, was designated as the first member of a new class of CA enzyme, δ -CAs (Cox et al. 2000, Roberts et al. 1997). Subsequent work using X-ray spectroscopy showed that, similar to α -CAs, the metal center in the active site of TWCA1 is also coordinated by the imidazole rings of three histidine residues (Cox et al. 2000). Recently, a close homolog of TWCA1 (50% identity at the amino acid level) was isolated and partially characterized from the coccolithophore *Emiliania huxleyi* (Soto et al. 2006). Interestingly, and unlike *Thalassiosira* species, the pennate diatom *Phaeodactylum tricoratum* appears to utilize β -CAs in photosynthesis and no evidence for δ -CAs has been found in this organism (Harada and Matsuda 2005, Satoh et al. 2001, Szabo and Colman 2007).

Phytoplankton can substitute Co for Zn in CA under Zn-limited conditions, which is critical under low CO₂ tensions when the requirement for CA is greatest (Lane and Morel 2000b, Sunda and Huntsman 1995, Yee and Morel 1996). Recently, a cadmium-containing CA has been isolated from the diatom *T. weissflogii*, which, at the present time, is the only known Cd metalloenzyme (Lane et al. 2005, CDCA1 is the first member of the newly designated ζ -class of CAs). In *T. weissflogii*, CDCA1 is composed of three nearly identical repeats yielding a functional enzyme of roughly 66 kDa molecular mass (Lane et al. 2005). The identification of CDCA1 provided an explanation for the observed ability of some diatoms to substitute Cd for Zn in a form of CA, which was clearly different from TWCA1 (Lane and Morel 2000a, Lee and Morel 1995, Morel et al. 1994, Price and Morel 1990). The requirement for Cd in CDCA1 also explained the apparent nutrient-like behavior of Cd in the surface ocean (Boyle et al. 1976). Indeed, recent evidence has shown that the CDCA gene is widely distributed in nature (Park et al. 2007, Park et al., submitted).

Similarity searches of the sequenced genome of the centric diatom *Thalassiosira pseudonana* revealed the presence of four TWCA1 homologs, ranging between 65 and 73% identity, and many other close homologs in a diverse range of marine phytoplankton gleaned from expressed sequence tag (EST) library searches. In contrast to CDCA1 of *T. weissflogii*, the homologous CDCA enzyme in *T. pseudonana* (CDCA_{TP}) is apparently a monomer of about 26 kDa (Lane et al. 2005). In this paper, we explored the regulation of both classes of CA by pCO₂ and trace metal status. We also present evidence for dynamic regulation of both forms of CA in natural phytoplankton assemblages sampled from the coast of New Jersey in the spring of 2007.

Materials and methods

Growth of phytoplankton

Stock cultures of *T. pseudonana* and *T. weissflogii* were typically maintained in f/2 medium under 20 $\mu\text{mol photons m}^{-2} \text{s}^{-1}$ and transferred into fresh f/2 once a month. Routinely, 'starter' cultures were grown where a small number of cells were transferred from stock cultures into trace-metal-buffered media in polycarbonate bottles under 90 $\mu\text{mol photons m}^{-2} \text{s}^{-1}$ continuous illumination. The medium was prepared from 0.2- μm filtered Gulf Stream water supplemented with major nutrients (10 $\mu\text{M PO}_4^{3-}$, 100 $\mu\text{M NO}_3^-$, 100 $\mu\text{M SiO}_2$), filter-sterilized vitamins and trace metals (20–80 nM Zn, 120 nM Mn, 0–50 nM Co, 20 nM Cu and 0.5–1 $\mu\text{M Fe}$) buffered with 100 $\mu\text{M EDTA}$ (Sunda et al. 2005). For experimental cultures, cells were transferred from starter cultures at a 1000-fold dilution into fresh growth medium containing various amounts of Zn in bottles that had been soaked overnight in 5% HCl. For some experiments, *T. pseudonana* cells were transferred into 'high pCO₂' media obtained by pre-bubbling growth media with air enriched to 1% CO₂ until the pH of the culture medium was 7.2. Phytoplankton growth in cultures was followed by enumerating cells with a Coulter counter (Beckman-Coulter, Fullerton, CA). Specific growth rates (day^{-1}) were determined by fitting linear regression curves to the natural log of cell number vs time.

Field samples were collected during two trips to the Rutgers University Marine Station at Tuckerton, New Jersey, in May and April 2007. The pH of the water was typically between 7.5 and 7.6, and the salinity was 3%. Chl *a* concentrations were typically around 1 $\mu\text{g l}^{-1}$. Briefly, approximately 20 l of water was pumped into a sterile polycarbonate carboy fitted with a Teflon spigot. The samples were transferred back to the laboratory in darkness, and aliquots were transferred into 1-l sterile polycarbonate bottles and illuminated at 90 $\mu\text{mol photons m}^{-2} \text{s}^{-1}$ from the bottom. To control pCO₂ levels, the pH was adjusted to either 7.4 or 8.3 by the addition of 5 mM 4-(2-hydroxyethyl)-1-piperazinepropanesulfonic acid (EPPS) buffer. In some bottles, no pH buffer was added. In bottles sampled from the first incubation (sampled 22 May 2007), the final pH values in the buffered bottles was 7.5 and 8.4. In the unbuffered bottle, the pH had risen to 8.8 and rose in the subsequent 24 h to 9.1. For the second incubation (20 April 2007), duplicate bottles were set up for each pCO₂ level and buffered with EPPS to final values of 7.44 and 7.37 for the low pH incubations and 8.24 and 8.30 for the higher pH incubations. The pH of the duplicate unbuffered bottles had risen to 8.16 in one and 8.44 in

the other. The bottles were incubated for 72 h (second incubation) or 100 h (first incubation) at which time 0.4–1 l samples were harvested on 10- μm polycarbonate filters under gentle vacuum. At the time of harvest, subsamples were assayed immediately for CA activity (see below) and the remainder was stored at -80°C for subsequent analysis of gene and protein expression.

CA assays

CA assays of *T. pseudonana* whole cells and phytoplankton collected from the field were conducted with the aid of a mass spectrometer attached through a membrane inlet to a thermo-regulated sample cell according to Miller et al. (1997). Briefly, *T. pseudonana* cells were collected on a 3- μm polycarbonate filter under gentle vacuum and resuspended in 1 ml of assay buffer (10 mM HEPES buffer, pH 8.2, 3.5% w/v NaCl). The cells were concentrated further by a brief spin in a benchtop centrifuge followed by removal of the supernatant and resuspension in 50 μl of assay buffer. The cell concentrates were snap-frozen in liquid N₂ and stored at -80°C until analysis, which was no more than 10 days from sampling. Just prior to snap-freezing, 10 μl of the concentrate was sampled and diluted into 10 ml of 3.5% NaCl and the cells enumerated directly by the Coulter counter. At the time of analysis, the cell pellets were thawed on ice and the remainder was directly injected into 0.96 ml of assay buffer containing 0.3–0.5 mM NaH¹³C¹⁸O¹⁸O in thermodynamic equilibrium with ¹³C¹⁸O¹⁸O (*m/z* = 49) at pH 8.2. The relative concentrations of *m/z* 49, *m/z* 47 (¹³C¹⁶O¹⁸O) and *m/z* 45 (¹³C¹⁶O¹⁶O) were followed over time and the ¹⁸O enrichment of ¹³C-labeled CO₂ was determined according to the following equation:

$$^{18}\text{O enrichment} = \log_{10} [49 / (49 + 47 + 45)] \times 100 \quad (1)$$

This relationship is linear with respect to time and the slope is directly proportional to the CA activity. At an enrichment value of 2, 100% of the ¹³C-labeled CO₂ is doubly labeled with ¹⁸O. At an enrichment value of 1, only 10% of the CO₂ remains doubly labeled. The assay measures the rate at which the enrichment falls from a value of 2 to 1, which is a function of the rate constants of CO₂ hydration and HCO₃⁻ dehydration in the assay medium. An external standard curve relating activity to the slope of the ¹⁸O enrichment curve was constructed using various amounts of bovine CA. The Y-intercept of this curve was taken as the enrichment slope determined in the absence of CA catalyst. Activities are reported here as Wilbur–Anderson units per 10⁸ cells or per mg Chl *a*.

Quantitative reverse transcriptase–polymerase chain reaction

Total RNA was isolated from diatoms with Trizol reagent (Invitrogen, La Jolla, CA) according to the suggested protocol. Cells (between 2×10^8 and 3×10^8 cells) were collected by gentle filtration and resuspended in 1 ml of Trizol in a sterile 50-ml Falcon tube. The extract was transferred to a sterile microfuge tube and heated to 65°C for 10 min. The extract was cooled to room temperature and 0.2 volumes of chloroform was added, followed by centrifugation at 12 000 *g* for 20 min to separate the aqueous and organic phases. The aqueous phase was collected by careful removal with a sterile pipette tip and transferred to a clean, sterile microfuge tube. The RNA was precipitated by adding an equal volume of isopropanol, mixing and centrifuging the mixture for 10 min at 12 000 *g*. The RNA pellet was washed with 75% ethanol, dried and resuspended in 20–30 μ l ultrapure deionized water. The purified RNA was treated with 2 units of DNase (Ambion, Austin, TX) to remove traces of genomic DNA. RNA was quantified by measuring absorbance at 260 nm in preparations diluted 200-fold.

First strand cDNA synthesis was carried out with 2 μ g of total RNA using the Superscript III kit (Invitrogen) according to the manufacturer's recommendations. Pools of cDNA were diluted five-fold with sterile deionized water before amplification on the quantitative reverse transcriptase–polymerase chain reaction (qRT-PCR) machine.

In this study, qRT-PCR analysis was used to quantify the abundance of several transcripts encoding CA enzymes. For laboratory experiment samples, transcript copy number was determined by comparison of the mean C_t value with a set of external DNA standards that were generated as follows. PCR products were generated for the genes of interest by amplifying cDNA prepared as described above in 25 μ l reactions containing 1 μ l of diluted cDNA product, 1.5 mM MgCl₂, 0.2 mM deoxyribonucleotide triphosphates, 12.5 pmol

each of forward and reverse primer and 1 unit of Taq polymerase (Roche, Indianapolis, IN). The PCR cycling program was 95°C for 1 min, followed by 35 cycles of 94°C for 15 s, 58°C for 20 s and 72°C for 30 s. Amplicons were separated on 2% agarose gels and visualized by ethidium bromide staining on a standard UV transilluminator. A single PCR product of the correct size was excised with a sterile razor blade and purified (Qiaex II gel extraction kit; Qiagen, Valencia, CA). The purified DNA was quantified with Picogreen (Picogreen dsDNA quantitation kit; Molecular Probes) and copy numbers per unit volume were determined. All quantitative polymerase chain reactions (qPCRs) were carried out on the Stratagene MX3000P thermal cycler instrument (Stratagene, La Jolla, CA). A Sybr-Green mastermix (Brilliant® SYBR® Green qPCR mastermix; Stratagene) was used for qPCR in 50 μ l reactions containing 3 μ l of diluted cDNA and 25 pmol each of forward and reverse primer using the following cycling program: 95°C for 10 min, followed by 40 cycles of 94°C for 15 s 58°C for 20 s and 72°C for 30 s. Standards corresponding to between 10^2 and 10^6 copies per well were amplified on the same 96-well plate as cDNA generated from experimental material. In order to correct for differences in RNA starting material and variations in cDNA synthesis efficiency (Parker and Armbrust 2005), the abundance of each transcript was normalized to the abundance of the actin transcript (Copies transcript of interest copy actin⁻¹), which was constitutively expressed in relation to changing pCO₂ or Zn status. All oligonucleotide sequences used in this study are listed in Table 1. For field samples, transcript abundance (RER for relative expression ratio) was expressed relative to the 18S rRNA expression, which was constitutive under varying pCO₂, according to the following equation:

$$\text{Relative transcript abundance} = 2^{(\Delta C_t)} \quad (2)$$

where ΔC_t represents the difference between the threshold cycle obtained for the internal reference transcript, in this case the gene encoding the 18S rRNA (C_t 18S),

Table 1. Oligonucleotide sequences for qRT-PCR analyses performed in this study.

Gene	Forward primer (5' → 3')	Reverse primer (5' → 3')	Fragment size (bp)
<i>twca_{TP1}</i>	atggcaacggtcctcatggaaatgttg	aatgtcttgcgccaagcgtagtga	308
<i>twca_{TP2}</i>	acggtagcgggtccaccaggtaacatc	accacagcagaggcgatattcctga	323
<i>twca_{TP3}</i>	gatcgctctgtagaagaggagcagcct	tgcatctgcaacagagtaaagagtgc	311
<i>twca_{TP4}</i>	aaccgaacactactccgagcgagta	catcaaatcaggatagaagtattctctctc	394
<i>cdca_{TP}</i>	gaggccatgatgacctccgtcgacgcctc	gtgacgctcgagcttctatcctgggtc	450
<i>Actin</i>	actggattggagatggatgg	caaagcgttaattctctctc	162
<i>twca</i> field	taygargtkcaytgccctca	cactyrcgrtckacctgcaaa	n.d.
<i>rbcl</i>	atgcgttgagagarcgtttctta	acaccwsacatcagcatccattaca	332

and that obtained for the gene of interest (Ct Target; *twca*, *cdca* or *rbcl*) according to Kustka et al. (2007).

Western blotting

The expression of δ -CAs and ζ -CAs in *T. pseudonana* cells and in field extracts and TWCA1 in *T. weissflogii* was assayed by immunoblot analyses using antisera raised against the TWCA1 protein and against a conserved polypeptide fragment of the CDCA enzyme (Roberts et al. 1997, Xu et al., unpublished data). Briefly, 50 μ l of cell concentrate was centrifuged for 5 min at 20 000 *g*. The supernatant was removed and 100 μ l of SDS loading buffer was added followed by a brief vortex. The extract was boiled for 5 min, centrifuged again and allowed to cool to room temperature. After cooling, a 50 μ l aliquot was removed for determination of total protein (see below). Equivalent amounts of total protein were loaded into each lane and separated on a 15% polyacrylamide gel for 35 min at 250 V in 1 \times SDS running buffer. A lane containing 7.5 μ l of protein molecular size standards was also run (Dual Colour Precision Plus Protein Standards; Bio-Rad Laboratories, Hercules, CA). After electrophoresis, proteins were transferred to polyvinylidene fluoride (PVDF) membrane in ice-cold transfer buffer [8 mM NaHCO₃, 2.4 mM Na₂CO₃, 20% methanol (v/v)] for 1 h at 200 mA. The membrane was blocked with 5% milk powder in TBST buffer (Tris-buffered saline containing 0.25% v/v Tween-20, pH 7.5) for 1 h at room temperature. The blocked membrane was probed for 1 h with 10–15 μ l of primary TWCA1 antisera or 2 μ l of CDCA antisera followed by five 5-min washes with TBST buffer to remove unbound antibody. After washing, the membrane was probed for 1 h with 1 μ l of alkaline phosphatase-linked, goat anti-rabbit immunoglobulin G (Sigma, St Louis, MO), followed by five washes with TBST buffer. The membrane was quickly washed twice with PhoA buffer (20 mM Tris, 100 mM NaCl and 10 mM MgCl₂, pH 9.5) and protein bands were visualized by adding 0.5% nitro-blue tetrazolium chloride/5-bromo-4-chloro-3'-indolylphosphate p-toluidine (NBT/BCIP) chromogenic alkaline phosphatase (APase) substrate in PhoA buffer. Bands usually developed within 10 min after addition of substrate. Bands from field samples were allowed to develop overnight.

Total protein determination

In order to remove potentially interfering cellular substances from the protein assay, total protein from 50 μ l denatured cell extracts was first precipitated with the Compat-Able Protein Assay kit (Pierce Biotechnology, Rockford, IL) according to the manufacturer's suggested

protocol. Precipitated protein was redissolved in 0.2 ml 2% SDS and the absorbance of the solution at 260 and 280 nm was read in a spectrophotometer. Total protein concentrations were estimated according to the following equation:

$$\text{Protein } (\mu\text{g ml}^{-1}) = (1.55 \times A_{260}) - (0.76 \times A_{280}) \quad (3)$$

Results

Phylogenetic analysis of δ -CAs from marine phytoplankton

At the present time, only two δ -CA enzymes have been isolated and characterized, TWCA1 (Roberts et al. 1997) and one from *E. huxleyi*, TWCA_{Eh} [designated δ -EhCA1 in Soto et al. (2006)]. BLAST searches of publicly accessible EST libraries revealed the presence of putative TWCA1 homologs in a surprisingly diverse range of phytoplankton (Fig. 1A). The δ -CA class would therefore appear to be commonly used in marine settings for inorganic carbon acquisition mechanisms, although we have limited information at present concerning the exact role played by TWCA in these phytoplankton species. A phylogenetic analysis of representative δ -CAs is presented in Fig. 1A in which three distinct clades become apparent (Table 2). The first clade is formed by the two haptophytic representatives, *E. huxleyi* and *Isochrysis galbana* along with two dinoflagellates *Lingulodinium polyedrum* and *Karenia brevis*. The second clade consists of the four putative TWCA1 homologs from *T. pseudonana* and TWCA1 itself. The third clade consists of the two prasino-phytes, *Ostreococcus lucimarinus* and *Micromonas* sp. as well as a third dinoflagellate, *Alexandrium tamarense*. Also presented is a short region of relatively high similarity between all 12 sequences that may provide insight into residues important for CA activity (Fig. 1B). This is described in more detail in the Discussion.

Zn limitation reduces growth rate and CA activity in *T. pseudonana*

Decreasing the free Zn concentration (Zn', unchelated form) from 20 to 5 pM in laboratory cultures decreased the specific growth rate of *T. pseudonana* from approximately 2 to 1.3 day⁻¹, a decrease remarkably similar to other studies (Fig. 2, Sunda and Huntsman 2005). In cultures under moderate CO₂ limitation (pH between 8.4 and 8.6), whole-cell CA activity decreased only slightly as Zn' levels were lowered from 20 to 7 pM, but dropped off sharply as the Zn' fell from 7 to 5 pM (Fig. 2, diamond symbols). During growth of phytoplankton in closed bottles, dissolved CO₂ levels fall as the rate of CO₂

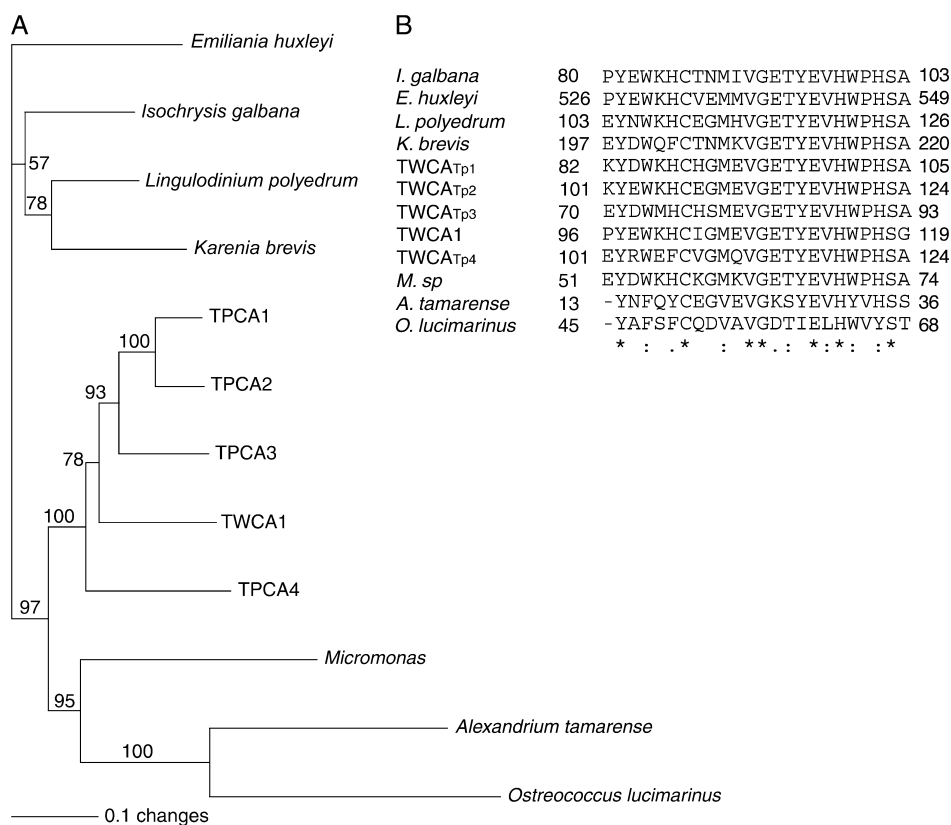


Fig. 1. Distribution of δ -CA (TWCA1-like) homologs in marine phytoplankton. (A) Phylogenetic analysis of deduced amino acid sequences of putative TWCA1 homologs. Sequences were generated by BLAST searches of EST databases (<http://www.ncbi.nlm.nih.gov/BLAST/>) and the genomic sequence of *Thalassiosira pseudonana* (<http://genome.jgi-psf.org/Thaps3/Thaps3.home.html>). Explanatory details for each EST are listed in Table 2. Sequences were aligned with CLUSTALW software using default gap extension and gap opening choices. PAUP 4.0 was used to generate a neighbor-joining distance tree. (B) Aligned region of high homology within the coding sequences of TWCA1 and its putative homologs (Discussion). '*' indicates residue is absolutely conserved, ':' indicates conservative substitution, '.' indicated less conservative substitution.

assimilation by the phytoplankton biomass exceeds the rate at which CO_2 is redissolved from the air from the headspace. This is seen as a rise in the pH of the culture during growth, which is augmented by the uptake of NO_3^- . We detected higher cellular CA activities in cultures harvested at lower CO_2 tensions (pH between 8.6 and 8.8) compared with cultures harvested under relatively higher CO_2 (pH between 8.4 and 8.6) (Fig. 2, compare diamond symbols with circle symbols). This

observation was true for cultures grown with 7, 9 and 20 $\mu\text{M Zn}'$ but was especially pronounced in the high-Zn cultures. Interestingly, the relative increase in CA activity between high and low CO_2 was greater in cultures that contained 7 $\mu\text{M Zn}'$, compared with 9 $\mu\text{M Zn}'$, although the absolute activities measured at these two Zn' levels under high and low CO_2 did not differ significantly. Unfortunately, no cultures containing 5 $\mu\text{M Zn}'$ were grown long enough to raise the pH above 8.6.

Table 2. Putative homologs of the δ -CA TWCA1 in marine phytoplankton revealed by BLAST similarity searches.

Phytoplankton species	Classification	GenBank Accession no.	E value	Alignment score	Identity to TWCA1 (%)
<i>Isochrysis galbana</i>	Prymnesiophytes	EC146599.1	7e-80	301	61 (149/243)
<i>Lingulodinium polyedrum</i>	Dinoflagellate	CD809592.1	7e-66	254	73 (119/162)
<i>Micromonas CCMP490</i>	Chlorophyte	EC47708.1	2e-50	176	57 (99/173)
<i>Karenia brevis</i>	Dinoflagellate	CO063433.1	7e-50	201	54 (78/142)
<i>Alexandrium tamarense</i>	Dinoflagellate	CK786473.1	4e-20	102	40 (40/172)
<i>Ostreococcus lucimarinus</i>	Chlorophyte	ES340888.1	1e-13	81	32 (59/179)

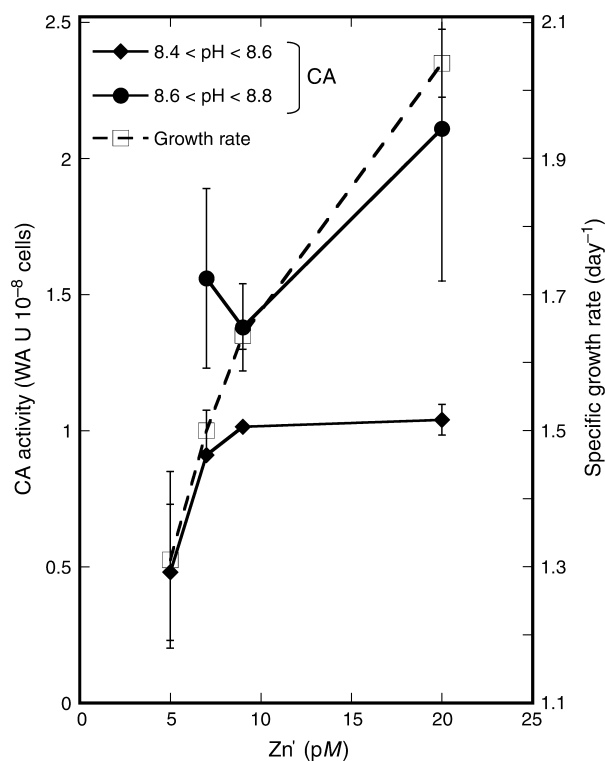


Fig. 2. Effect of Zn limitation on specific growth rate and CA activity in the marine diatom *Thalassiosira pseudonana*. For CA activity measurements, cultures were harvested within a range of two different pCO₂: when the medium pH was between 8.4 and 8.6 (filled diamond symbols) and when the pH was between 8.6 and 8.8 (filled circle symbols). Details of the assay are given in Materials and methods. Points are the means of at least three biological replicates and the error bars represent 1 SD about the mean.

Western blot analysis of diatom CAs – Zn limitation reduces CA expression

Antisera raised against TWCA1 were used to probe protein extracts isolated from Zn-replete and Zn-limited *T. pseudonana* cells. As a positive control, a *T. weissflogii* extract was also probed with this antibody (Fig. 3, lane 1). In the positive control lane, TWCA1 was detected at 25 kDa, which was slightly smaller than the reported size of 27 kDa (Roberts et al. 1997). We detected apparent TWCA1 homologs in *T. pseudonana* extracts, notably an intense band of approximately 24 kDa in the high-Zn treatment, which appeared to be strongly downregulated in the low-Zn treatment (Fig. 3A, lanes 2 and 3). This size corresponds roughly to the predicted sizes of TWCA_{TP1} and TWCA_{TP2} based on their deduced amino acid sequences of 263 and 277 amino acids, respectively, and therefore likely represents simultaneous detection of these two CAs. Other bands at approximate sizes of 30, 22, 19 and 17 kDa were detected in both high and

low-Zn extracts (Fig. 3A, arrows.) The three smaller bands appeared to be slightly more abundant in the high-Zn extracts. Whether or not these represent other forms of δ-CA or were detected non-specifically by the antibody is unknown at present. Clearly, the Zn concentration strongly influences the abundance of δ-CAs in *T. pseudonana*.

We also performed Western blot analysis with CDCA antisera using extracts of cells from which the CA activity measurements were made (Fig. 2) in order to study the potential for Zn to regulate the expression of CDCA enzyme in *T. pseudonana*. Surprisingly, we detected a strong effect of Zn on the abundance of the 26-kDa CDCA enzyme in *T. pseudonana* (a monomer, Fig. 3B). Limiting the growth rate with Zn caused a systematic decrease in CDCA_{TP} protein abundance from Zn-replete cells (20 pM Zn²⁺) to the most severely limited (5 pM Zn²⁺, Fig. 3B). This result was unexpected and appears at odds with the results obtained with *T. weissflogii* (Lane and Morel 2000a, Park et al., submitted). As discussed below, *T. pseudonana* and *T. weissflogii* may use different metals in CDCA.

Transcript analysis 1 – regulation of CA transcripts by zinc and cobalt

We conducted qPCR analyses of individual *twca*_{TP} and *cdca*_{TP} transcripts in cells grown under different Zn levels in media where the CO₂ level was initially in equilibrium with air in order to more fully explore the dynamic regulation of these genes as a function of trace metal status (pH 8.3, RNA was isolated from the same cells as those used for CA activity measurements shown in Fig. 2). The *twca*_{TP1} transcript abundance decreased approximately eight-fold from Zn-replete cells to the most Zn-limited cells (Fig. 4A). *Twca*_{TP2} expression appeared to be more resistant to Zn limitation as we detected no significant changes in the abundance of this transcript in cells when the growth rate was reduced by up to 25% (Fig. 4A). In the most Zn-limited cells, however, the abundance of *twca*_{TP2} decreased approximately 2.5-fold compared with Zn-replete cells (Fig. 4A). Somewhat surprisingly, and in contrast to *twca*_{TP1} and *twca*_{TP2}, *twca*_{TP3} and *twca*_{TP4} transcripts increased in abundance as Zn became more limiting for growth (Fig. 4B).

In parallel with the expression of *twca*_{TP1} and *twca*_{TP2}, and in agreement with the results of the Western blot analysis from Fig. 3B, we observed a strong regulatory effect of Zn on the expression of the *cdca* transcript in *T. pseudonana*. *Cdca*_{TP} transcript abundance fell by approximately 2.5-fold going from Zn-replete cells to the most Zn-limited cells (Fig. 4A, dashed line). The *cdca*_{TP} transcript was more abundant than any of the *twca*_{TP}

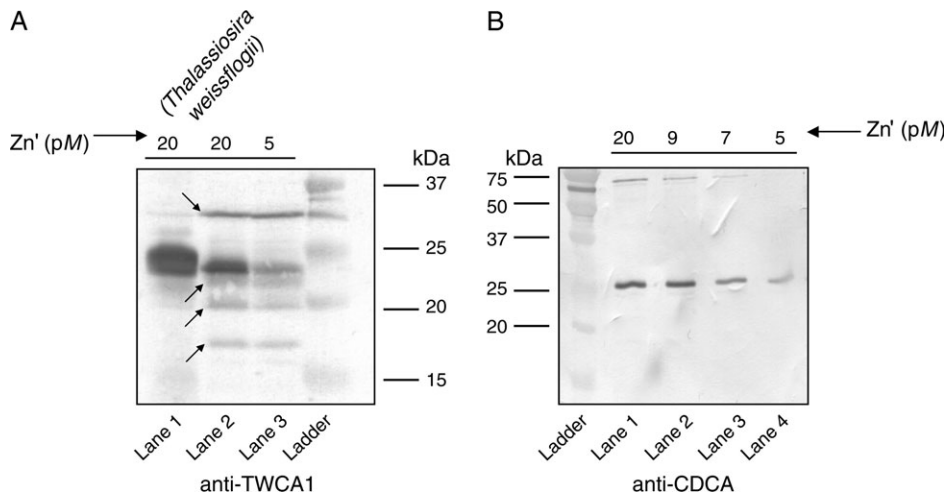


Fig. 3. (A) Western blot analysis of the effect of Zn on TWCA_{TP} and (B) CDCA_{TP} expression in the marine diatom *Thalassiosira pseudonana*. For the CDCA_{TP} detection, protein extracts were prepared from the same cultures from which the growth rates and CA activity assays were determined (Fig. 2).

transcripts. The results of the qRT-PCR analysis for *cdca*_{TP} were remarkably consistent with that of the Western blot analysis using CDCA antisera (Fig. 3B).

We also explored the expression patterns of *twca*_{TP1-4} and *cdca*_{TP} in Zn-limited cells cultured with either low or

high levels of Co (Table 3). In some phytoplankton, cobalt can substitute efficiently for Zn in CA when the latter is limiting and so we sought to determine whether this substitution also occurs in *T. pseudonana* (Lane and Morel 2000a). In the presence of 5 pM Zn²⁺ and 2.1 pM

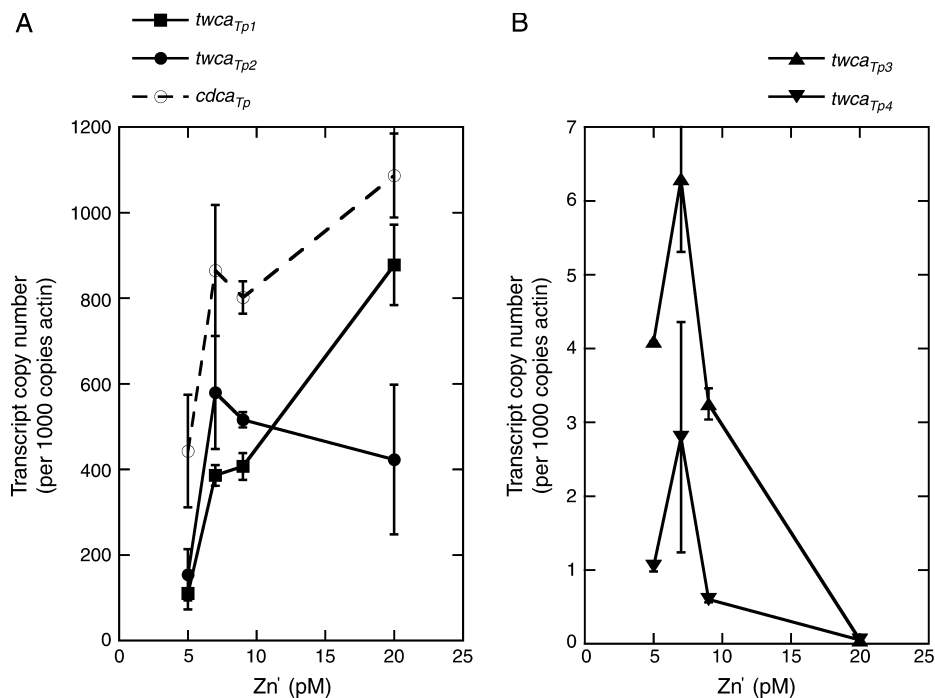


Fig. 4. qRT-PCR analysis of the effect of Zn on steady-state levels of transcripts encoding *twca*_{TP} and *cdca*_{TP} in *Thalassiosira pseudonana*. (A) Transcripts encoding *twca*_{TP1} (filled squares), *twca*_{TP2} (filled circles) and *cdca*_{TP} (open circles). (B) Transcripts encoding *twca*_{TP3} (filled triangles) and *twca*_{TP4} (inverted triangles). All CA transcripts were normalized to the actin transcript, which was constitutively expressed under Zn limitation. For this analysis, total RNA was extracted from the same cultures from which the growth rates and CA activity assays were determined (Fig. 2). Points are the means of three separate biological replicates. Error bars represent 1 SD about the mean.

Table 3. Effect of Co' on the growth rate, CA activity and transcript expression in Zn-limited cells of the marine diatom *Thalassiosira pseudonana*. Transcript abundance is reported in units of copies per 1000 copies of the actin reference transcript.

Parameter	Co' (pM)	
	2	20
Specific growth rate (day^{-1})	1.30	1.38
Relative CA activity	1.0	1.3
$twca_{TP1}$	374	558
$twca_{TP2}$	597	834
$twca_{TP3}$	6.4	0.2
$twca_{TP4}$	1.1	0.2
$cdca_{TP}$	950	1134

Co' , the specific growth rate was 1.30 day^{-1} , which increased to 1.38 day^{-1} when Co' was increased to 21 pM. This mild stimulation of growth in this unduplicated experiment was accompanied by a 31% increase in whole-cell CA activity (Table 3). At the level of transcripts, both $twca_{TP1}$ and $twca_{TP2}$ increased in abundance by approximately 1.5- and 1.7-fold, respectively, in the faster growing Zn-limited cultures amended with 21 pM Co' , relative to low- Co' cultures. In contrast, $twca_{TP3}$ and $twca_{TP4}$ transcripts decreased by approximately 30- and six-fold, respectively, under these conditions. In a pat-

tern similar to that observed for $twca_{TP1}$ and $twca_{TP2}$, $cdca_{TP}$ transcript abundance increased by approximately 1.2-fold in Zn-limited cells amended with 21 pM Co' (Table 3).

Transcript analysis 2 – regulation of CA transcripts by pCO_2

We also quantified the abundance of $twca_{TP}$ and $cdca_{TP}$ transcripts in Zn-replete cells grown under high or low CO_2 (Fig. 5). In this experiment, the growth medium was preconditioned to high CO_2 by a brief aeration with 1% CO_2 to lower the pH to 7.2. For the low- CO_2 treatment, the growth medium was initially air equilibrated at pH 8.3 and became CO_2 limited as the culture grew and the pH was driven up to 8.9. The expression of the $twca_{TP1}$ and $twca_{TP2}$ transcripts was strongly regulated by CO_2 growth regimen (Fig. 5A). In high- CO_2 media, we measured 6 ± 4 and 4 ± 2 copies ($n = 3$) of the $twca_{TP1}$ and $twca_{TP2}$ transcript, respectively, for every 1000 copies of the actin transcript (Fig. 5A). In low- CO_2 -grown cells, this ratio increased to 1240 ± 260 and 600 ± 140 copies, respectively, for these two transcripts ($n = 3$, Fig. 5A). Both $twca_{TP3}$ and $twca_{TP4}$ transcripts were much more weakly expressed than $twca_{TP1}$ or $twca_{TP2}$ under both CO_2 growth regimens (Fig. 5B). However, we detected a modest increase in $twca_{TP3}$ abundance from 1.6 ± 0.4

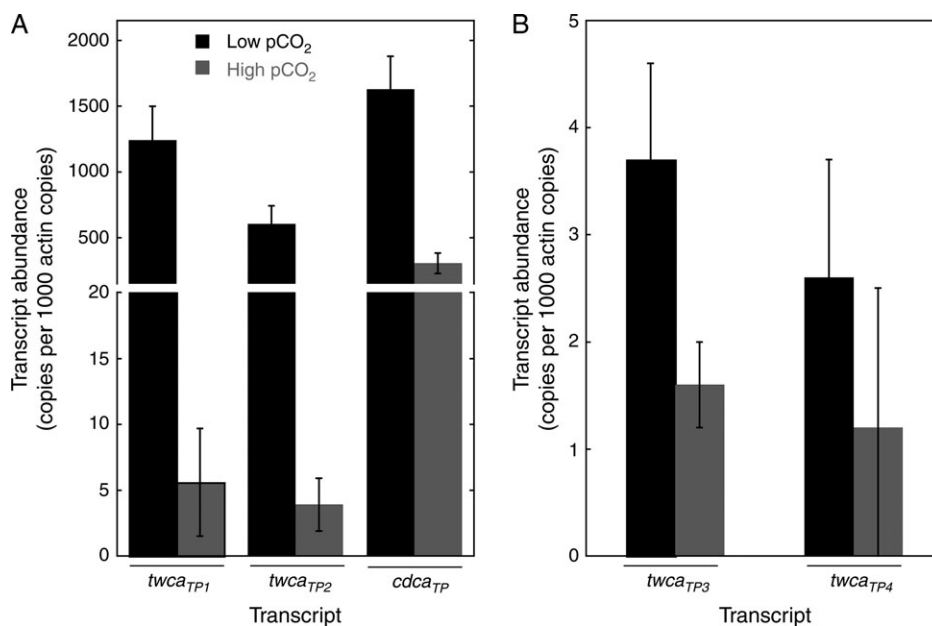


Fig. 5. qRT-PCR analysis of the effect of pCO_2 on steady-state levels of transcripts encoding $twca_{TP}$ and $cdca_{TP}$ in *Thalassiosira pseudonana*. (A) Transcripts encoding $twca_{TP1}$, $twca_{TP2}$ and $cdca_{TP}$. (B) Transcripts encoding $twca_{TP3}$ and $twca_{TP4}$. Points are the means of three separate biological replicates. All CA transcripts were normalized to the actin transcript, which was constitutively expressed under these conditions. Error bars represent 1 SD about the mean. Mean specific growth rates for cultures grown under low and high pCO_2 were 1.98 ± 0.02 and $2.05 \pm 0.1 \text{ day}^{-1}$, respectively ($n = 3$).

in high-CO₂ cells to 3.7 ± 1 copies in low-CO₂ cells, per 1000 copies of actin. No significant effects of CO₂ growth regimen on *twca*_{TP4} abundance were observed (Fig. 5B).

Again, we detected strong regulation of about six-fold in *cdca*_{TP} expression by pCO₂ under Zn-replete conditions (Fig. 5A). As was the case for the Zn limitation experiments (Fig. 4, Table 2), the *cdca*_{TP} transcript was more abundantly expressed than any other CA transcript. Particularly striking is the abundance of the *cdca*_{TP} transcript under high pCO₂, when none of the three primary environmental modulators of CA expression, namely pCO₂, Zn and Co, were limiting the growth rate (Fig. 5A). Under high pCO₂, *cdca*_{TP} transcript abundance approaches the abundance of *twca*_{TP2} under low pCO₂. In addition to its susceptibility to regulation by Zn in the absence of Cd (Figs 3B and 4A), *cdca*_{TP} is also strongly regulated under conditions where only CO₂, and not Zn, was limiting (Fig. 5A).

Detection of diatom CAs in the field

Results from the laboratory showed strong regulation of the complement of TWCA_{TP} and CDCA_{TP} by pCO₂, Zn and Co concentrations. We sought to explore the regulation of these CA classes in a field setting to compare with our results obtained in controlled laboratory conditions. Un-

fortunately, the high concentrations of Zn and Cd found at the sampling site (0.8 ppb total Zn and 0.04 ppb total Cd maxima, Field et al. 1999) prevented us from conducting any experiments to examine the effect of trace metal additions on CA expression in these waters. The standing phytoplankton biomass was typically around 1 μg Chl a l⁻¹ and microscopic examination revealed the community to be overwhelmingly dominated by large centric and chain-forming diatoms, with a minor numerical contribution from dinoflagellates (data not shown).

In the first incubation experiment, whole-cell CA activity measurements with the membrane inlet MS were conducted on incubated phytoplankton assemblages as well as qRT-PCR analysis of CA transcript expression. We detected a four-fold increase in CA activity in the >10 μm phytoplankton community as the pH increased from 7.4 to 9.1 in the incubation bottles (Fig. 6A). From the same samples, we isolated total RNA and performed qRT-PCR analyses of *twca* and *cdca* transcript abundances using primers designed against conserved amino acids identified by multiple sequence alignment of members from both classes. We comonitored the abundance of transcripts encoding the large subunit of RubisCO. In the pH range of 7.4–8.8, the CA activity increased by about three-fold: correspondingly the *cdca* transcript increased by a factor of 2, while *twca* transcripts remained more or less

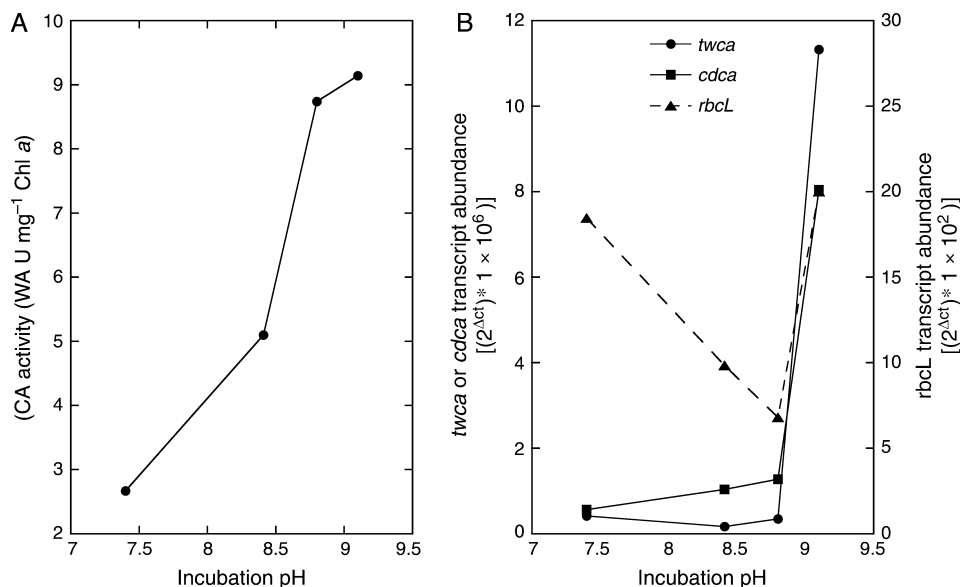


Fig. 6. Effect of pCO₂ incubation on (A) CA activity and (B) *twca*, *cdca* and *rbcL* transcript expression from field samples taken from Great Bay, New Jersey in May 2007. Twenty liters of samples was taken and subsampled into 1 l polycarbonate bottles. Inorganic pH buffer (5 mM EPPS) was added to final pH of 7.4 and 8.3 to maintain pCO₂ constant during the incubation. In these bottles, the pH at the time of harvest was 7.4 and 8.41, respectively. In a third bottle, omission of EPPS allowed the pCO₂ to increase as the phytoplankton grew. In this bottle, the pH increased to 8.8 after 80 h of incubation and increased to 9.1 in the subsequent 24-h period. At the point of harvest, >10-μm-diameter phytoplankton were collected by gentle filtration and concentrated in buffer. An aliquot was assayed immediately for CA activity by membrane inlet mass spectrometry. The remainder was added to 1 ml of Trizol reagent for extraction of total RNA for qRT-PCR analysis. Chl content was determined by extraction in 100% methanol.

constant. In the range of pH 8.8–9.1, there was only a modest increase in CA activity but a large increase in both *cdca* and *twca* transcript abundance (Fig. 6B). RubisCO large subunit abundance decreased somewhat as the pH increased to 8.4 and 8.8 and then subsequently rose again as the pH went above 9.0.

In the second incubation, Western blot analyses from phytoplankton extracts probed with CDCA antisera revealed an approximately 26-kDa immunoreactive band of the same size detected from *T. pseudonana* extracts, suggesting that the CDCA monomer was the dominant form expressed in this community (Fig. 7). In a similar fashion to the results obtained in the laboratory (Fig. 5A), CDCA appeared to be tightly regulated by $p\text{CO}_2$ in this natural community, with weak expression seen in the high $p\text{CO}_2$ incubations and stronger expression seen as the pH was raised and the CO_2 decreased. There appeared to be a strong positive correlation between the expression of CDCA and the incubation pH (which reflects the $p\text{CO}_2$). The same extracts probed with TWCA1 antisera did not reveal any bands on the immunoblot (data not shown), suggesting either that this class is not sufficiently expressed in this community to be detected or that the antibody we used does not broadly recognize members of the δ -CA class outside of TWCA1 and *TWCA_{TP}*.

Discussion

The distribution of the δ -CA class in marine phytoplankton

Our search for TWCA1 homologs has increased the number of known δ -CAs from two (namely TWCA1 and an apparent *TWCA_{EH}* in *E. huxleyi*, Soto et al. 2006) to 12. Although in *T. pseudonana*, we have not proved that these genes encode functional CAs, for instance by

cloning and overexpressing recombinant forms and measuring the resultant activity, their high identity scores to TWCA1 coupled with their tight regulation by $p\text{CO}_2$, Zn and Co strongly suggest that they are genuine TWCA enzymes. This paper is the first to describe the regulation by multiple factors of multiple CAs in both monocultures and mixed phytoplankton communities from field samples.

Unlike the ζ -CAs, which appear to be confined to diatoms, the δ -CA class of CAs is widely distributed in marine phytoplankton. It is found in members of those Chl *a*- and Chl *a c*-containing groups, which make up the prymnesiophytes (haptophytes), heterokonts and the chlorophytic prasinophytes. BLAST searches of EST libraries revealed TWCA1 homologs in an abundance of marine phytoplankton, spanning a wide phylogenetic range (Fig. 1A, Table 2). The sequences from the two prymnesiophytes representatives, *E. huxleyi* and *I. galbana*, appear to be the closest non-diatom homologs to TWCA1. In phytoplankton that is more distantly related to diatoms, such as the marine chlorophytes *O. lucimarinus* and *Micromonas* sp., the degree of homology to TWCA1 was conspicuously lower (Table 2). Three dinoflagellate species were also found to possess homologs of varying similarity to TWCA1 (Table 2). The symbiotic dinoflagellate *Symbiodinium* has also been reported to contain at least one homolog to TWCA1 (David Yellowlees, personal communication). Our analysis presented here would strongly suggest that the phylogeny of δ -CA genes is likely to be congruent with the 18S rDNA phylogenetic marker or perhaps other plastid-based markers of phylogeny and that all extant δ -CA genes share a common ancestor. This in turn implies that the appearance of this particular class of CA must have predated the divergence of the 'green' and 'red' phytoplankton lineages and therefore must be quite ancient indeed (Falkowski et al. 2004).

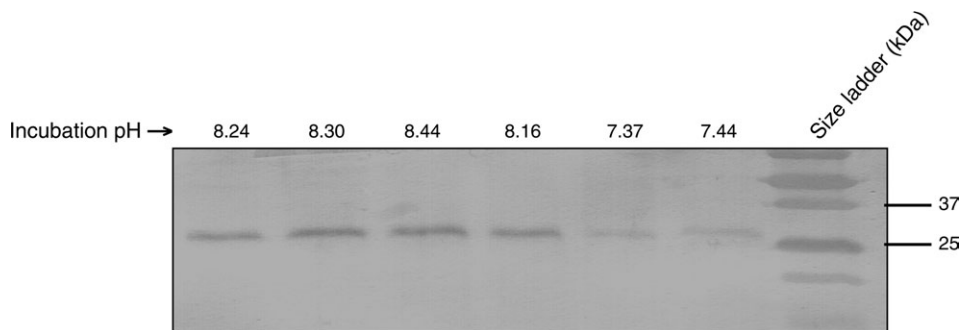


Fig. 7. Effect of 72-h incubation at various $p\text{CO}_2$ on CDCA abundance in field samples taken from Great Bay, New Jersey in April 2007. Conditions of sampling, incubation and harvesting were the same as that described for Fig. 6. Immunoblot probed with CDCA antiserum showing apparent monomeric CDCA band of about 26 kDa detected in protein extracts incubated at different $p\text{CO}_2$.

Conserved motifs in TWCA homologs

Although the degree of homology to TWCA1 in the more divergent sequences was low (<40% identity in *Alexandrium* and *Ostreococcus*, Table 1), a localized region of 23 amino acids of relatively high homology was identified within the coding sequences (Fig. 1B). Thirteen residues were either absolutely conserved or conserved in all but the *Ostreococcus* and/or *Alexandrium* sequences. In all but these two more divergent sequences, the conserved motif VGETYEVHWP \mathbf{H} S was especially conspicuous. Of particular interest was the presence of the two conserved histidine residues therein (H105 and H108 in bold, numbering with respect to TWCA1), which could serve as two of the three histidines thought to compose the Zn coordination site in the active site of the enzyme (Cox et al. 2000). A third histidine (H226) is conserved in all but the *K. brevis* sequence (data not shown), which could serve as the third active site residue, but this supposition awaits experimental verification using recombinant forms of the enzyme mutated at these key residues. At any rate, the similarity of this region between the 12 different sequences strongly suggests that it is important in terms of metal coordination and catalytic activity.

Regulation of CAs in *T. pseudonana*

In this paper, we present clear evidence for the regulation of both δ - and ζ -classes of CA in pure cultures of *T. pseudonana* by Zn, Co and pCO₂. In laboratory experiments where the growth rate was limited by low Zn, we observed concomitant reductions in CA activity and decreased abundance of TWCA_{TP} and CDCA_{TP} enzymes, which was reflected by a strong downregulation of *cdca*_{TP} and the main *twca*_{TP} transcripts. The pCO₂ was observed to exert a strong regulatory effect on the levels of both *twca*_{TP} and *cdca*_{TP} transcripts in the classical way: low pCO₂ stimulated a strong expression of these genes.

In the field, as in the laboratory, we observed dynamic regulation of CA expression at both the level of transcript and protein in natural phytoplankton assemblages to a similar degree as in the laboratory. Because of the high background concentrations of Zn and Cd at this field site (Field et al. 1999), we were not able to conduct experiments to look at the effect of trace metal additions on CA expression directly. But we clearly demonstrate a strong modulating effect of pCO₂ on the expression of both *twca* and *cdca*, the latter at the level of transcript and protein, which was similar in magnitude and direction as that seen in pure cultures of *T. pseudonana*. For reasons that are not clear, however, the strong upregulation of CA expression indicated by the transcript abundance was not

reflected by a proportionate increase in CA activity in the first incubation, although activity did increase (Fig. 6).

Our failure to detect TWCA forms in the field most likely reflects the inadequacies of the antibody, rather than true absence of this CA class from the environment. This antibody was raised against the purified full-length TWCA1 protein and therefore may not recognize homologous enzymes as efficiently (Roberts et al. 1997). By contrast, the antibody to CDCA was raised against a conserved region of the protein present in many isoforms and therefore potentially more likely to detect a broader phylogenetic range of the enzyme, which is especially important for field studies. Efforts are currently underway to identify potentially antigenic peptide sequences from conserved regions of TWCA1 suitable for raising antibodies against for use in field studies.

Metal replacement in diatom CAs

Our data support the idea that Co may substitute for Zn in TWCA_{TP} as has been shown for *T. weissflogii* (Lane and Morel 2000b). Cobalt had a similar effect on the expression pattern of *twca*_{TP} transcripts as Zn did (Table 3). Under low Zn and Co, *twca*_{TP1} and *twca*_{TP2} transcripts were depressed and *twca*_{TP3} and *twca*_{TP24} transcripts were elevated relative to Zn-replete conditions. When Co was supplied at non-limiting conditions under persistently low Zn, which boosted both the growth rate and the CA activity, *twca*_{TP1} and *twca*_{TP2} transcription increased and *twca*_{TP3} and *twca*_{TP4} transcription declined to levels approaching those observed under Zn repletion. However, it is important to point out that the degree to which Co substitutes for Zn in CA appears to be species dependent. For instance, Lane and Morel (2000b) were able to recover maximal growth rates and CA activity in Zn-limited *T. weissflogii* cells amended with 21 pM Co', compared with Zn-replete cells, indicating essentially complete replacement of Zn by Co. Despite the relatively robust growth rate of 1.3 day⁻¹ at a free Zn' concentration of 5 pM (Fig. 2), we were unable to get consistent growth below this value (data not shown). Indeed, growth was slow or negligible in cultures to which no Zn was added, even when the medium was supplemented with 21 pM Co' (data not shown). This indicates that, unlike *T. weissflogii* (Lane and Morel 2000b), *T. pseudonana* has an indispensable Zn requirement for which Co cannot substitute. In our study, the maximal growth rate observed in Zn-limited *T. pseudonana* cells amended with 20 pM Co' was only 65% of the Zn-replete growth rate, indicating incomplete replacement in this species (further addition of Co' did not increase growth rate). This is similar to the results of Sunda and Huntsman (1995), who observed approximately 60% replacement of Zn by Co in

the same species (specific growth rates of 0.85 in Co replete vs 1.43 in Zn-replete cells). *T. pseudonana* has also been shown to substitute Cd for Zn less efficiently than *T. weissflogii* (Lee and Morel 1995, Price and Morel 1990). Taken together, these results suggest that the degree to which Cd and/or Co can substitute for Zn in the field may depend on the phytoplankton community encountered.

The CDCA enzyme is the only known Cd metalloenzyme (Lane et al. 2005). In phytoplankton, the evolution of CDCA has been interpreted as a strategy to avoid growth limitation by CO₂ when Zn availability constrains phytoplankton capacity for CA synthesis (Lane and Morel 2000a). The implication of this somewhat limited role for CDCA is that its expression should be confined to a fairly narrow range of environmental conditions, namely low Zn, low pCO₂ and the presence of Cd levels sufficiently high to at least meet the demands of CDCA itself. The near-perfect replacement of TWCA1 by CDCA1 in *T. weissflogii* in the face of severe Zn limitation and added Cd argues in favor of this highly specialized role (Lane and Morel 2000a, Yee and Morel 1996). However, our results from the laboratory and the field would suggest that CDCA is expressed (and presumably active) under a much broader range of environmental conditions than one would predict from the above discussion. Under conditions of increasing Zn limitation that reduced growth rate, CA activity and TWCA_{TP} expression (Figs 2 and 3A, respectively), CDCA_{TP} expression was also strongly reduced at both the level of protein and transcript (Figs 3B and 4A, respectively). Clearly, under these conditions, CDCA expression is regulated by the same environmental parameters as TWCA in *T. pseudonana*.

Rather puzzling, however, is how to reconcile the evidence for an apparently robust expression of a presumably active CDCA enzyme under conditions of Zn and CO₂ limitation with the fact that, at least in the laboratory experiments, no Cd was added to the growth medium. The surprising result of the regulation of CDCA_{TP} by Zn is most likely explained by the new results of Xu et al. (submitted manuscript) who have shown in overexpression experiments that CDCA_{TP} can actually use Zn, as well as Cd, as a metal cofactor yielding a recombinant enzyme of extremely high activity. In light of these new data, our results would imply that, under the conditions of our experiments in *T. pseudonana*, the CDCA is likely functioning as a Zn enzyme. Indeed, the strong regulation by pCO₂ of CDCA in the coastal waters where the Zn concentration has been shown to be 30–40 times the Cd concentration (Field et al. 1999) suggests that it functions as a Zn enzyme under these conditions as well.

Unexpectedly, Co amendment increased the abundance of *cdca*_{TP} transcripts in Zn-limited *T. pseudonana* by approximately 1.2-fold in a trend, which matched the pattern seen with *twca*_{TP1} and *twca*_{TP2}. The enhancing effects of Co on CDCA_{TP} expression may imply that it is able to use Co, as well as Cd and Zn, as a metal center. The results of Xu et al. (submitted manuscript) showing facile metal exchange in its active site suggest that this is a possibility.

Conclusions

The evidence presented here argues strongly for coordinated regulation of δ- and ζ-CA classes in the marine diatom *T. pseudonana* and in natural phytoplankton assemblages by trace metals and pCO₂. Particularly striking was the strong correlation of diatom growth rate, availability of free Zn and/or Co and the cellular CA activity. This serves to highlight the important role played by trace metals in the biogeochemical cycling of carbon in marine environments. Our data also support the idea that CDCA is a 'cambialistic' enzyme in that it may function with either Zn or Cd as cofactor, depending on the relative concentrations of each metal in a particular environment.

Acknowledgements – The authors thank Rose Petrecca of the Rutgers University Marine Station for assistance with field sampling. We also thank the reviewers for their comments and suggestions. This work was supported by NSF grant OCE-0351499 and by the Center for Environmental Bioinorganic Chemistry (NSF grant 022197).

References

- Badger MR (2003) The role of carbonic anhydrases in photosynthetic CO₂ concentrating mechanisms. *Photosynth Res* 77: 83–94
- Badger MR, Andrews TJ, Whitney SM, Ludwig M, Yellowlees DC, Leggat W, Price GD (1998) The diversity and co-evolution of RubisCO, plastids, pyrenoids and chloroplast based CO₂ concentrating mechanisms in algae. *Can J Bot* 76: 1052–1071
- Boyle EA, Sclater F, Edmond JM (1976) On the marine geochemistry of cadmium. *Nature* 263: 42–44
- Cox EH, McLendon GL, Morel FMM, Lane TW, Prince RC, Pickering IJ, George GN (2000) The active site structure of *Thalassiosira weissflogii* carbonic anhydrase 1. *Biochem* 39: 12128–12130
- Falkowski PG, Katz ME, Knoll AH, Quigg A, Raven JA, Schofield O, Taylor FJR (2004) The evolution of modern phytoplankton. *Science* 305: 354–360
- Field MF, Cullen JT, Sherrell RM (1999) Direct determination of 10 trace metals in 50 μL samples of coastal seawater

- using desolvating micronebulization sector field ICP-MS. *J Anal At Spectrom* 14: 1425–1431
- Harada H, Matsuda Y (2005) Identification and characterization of a new carbonic anhydrase in the marine diatom *Phaeodactylum tricornutum*. *Can J Bot* 83: 909–916
- Hatch MD, Burnell JN (1990) Carbonic anhydrase activity in leaves and its role in the first step in C4 photosynthesis. *Plant Physiol* 93: 825–828
- Hewett-Emmett D, Tashian RE (1996) Functional diversity, conservation and convergence in the evolution of α -, β - and γ -carbonic anhydrase gene families. *Mol Phylogenet Evol* 5: 550–577
- Kaplan A, Reinhold L (1999) CO₂-concentrating mechanisms in photosynthetic microorganisms. *Annu Rev Plant Physiol Plant Mol Biol* 50: 539–570
- Kustka AB, Allen AE, Morel FMM (2007) Sequence analysis and transcriptional regulation of iron acquisition genes in two marine diatoms. *J Phycol* 43: 715–729
- Lane TW, Morel FMM (2000a) A biological function for cadmium in marine diatoms. *Proc Natl Acad Sci USA* 97: 4627–4631
- Lane TW, Morel FMM (2000b) Regulation of carbonic anhydrase expression by zinc, cobalt and carbon dioxide in the marine diatom *Thalassiosira weissflogii*. *Plant Physiol* 123: 345–352
- Lane TW, Saito MA, Georget GN, Pickering IJ, Prince RC and Morel FMM (2005) A cadmium enzyme from a marine diatom. *Nature* 435: 42
- Lee JG and Morel FMM (1995) Replacement of zinc by cadmium in marine phytoplankton. *Mar Ecol Prog Ser* 127: 305–309
- McGinn PJ, Morel FMM (2008) Expression and inhibition of the carboxylating and decarboxylating enzymes of the C4 photosynthetic pathway in marine diatoms. *Plant Physiol* (in press)
- Miller AG, Salon C, Espie GS, Canvin DT (1997) Measurement of the amount and isotopic composition of the CO₂ released from the cyanobacterium *Synechococcus* UTEX625 after rapid quenching of the CO₂ transport system. *Can J Bot* 75: 981–997
- Morel FMM, Reinfelder JR, Roberts SB, Chamberlain CP, Lee JG, Yee D (1994) Zinc and carbon co-limitation of marine phytoplankton. *Nature* 369: 740–742
- Morel FMM, Cox EH, Kraepiel AML, Lane TW, Milligan AJ, Schaperdoth I, Reinfelder JR, Tortell PD (2002) Acquisition of inorganic carbon by the marine diatoms *Thalassiosira weissflogii*. *Funct Plant Biol* 29: 301–308
- Park H, Song B, Morel FMM (2007) Diversity of cadmium-containing carbonic anhydrase in marine diatoms and natural waters. *Environ Microbiol* 9 403–413
- Parker MS, Armbrust EV (2005) Synergistic effects of light, temperature, and nitrogen source of transcription of genes for carbon and nitrogen metabolism in the centric diatom *Thalassiosira pseudonana* (Bacillariophyceae). *J Phycol* 41: 1142–1153
- Price NM, Morel FMM (1990) Cadmium and cobalt substitution for zinc in a marine diatom. *Nature* 344: 658–660
- Reinfelder JR, Kraepiel AML, Morel FMM (2000) Unicellular C4 photosynthesis in a marine diatom. *Nature* 407: 996–999
- Reinfelder JR, Milligan AJ, Morel FMM (2004) The role of the C4 pathway in carbon accumulation and fixation in a marine diatom. *Plant Physiol* 135: 2106–2111
- Roberts SB, Lane TW, Morel FMM (1997) Carbonic anhydrase in the marine diatom *Thalassiosira weissflogii* (Bacillariophyceae). *J Phycol* 33: 845–850
- Roberts K, Granum E, Leegood RC, Raven JR (2007) C3 and C4 pathways of photosynthetic carbon assimilation in marine diatoms are under genetic, not environmental, control. *Plant Physiol* 145: 230–235
- Satoh D, Hiraoka Y, Colamn B, Matsuda Y (2001) Physiological and molecular characterization of intracellular carbonic anhydrase from the marine diatom *Phaeodactylum tricornutum*. *Plant Physiol* 126: 1459–1470
- Soto AR, Zheng H, Shoemaker D, Rodriguez J, Read BA, Wahlund TM (2006) Identification and preliminary characterization of two cDNAs encoding unique carbonic anhydrases from the marine alga *Emiliania huxleyi*. *Appl Environ Microbiol* 72: 5500–5511
- Sunda WG, Huntsman SA (1995) Cobalt and zinc interreplacement in marine phytoplankton: Biological and geochemical implications. *Limnol Oceanogr* 40: 1404–1417
- Sunda WG, Huntsman SA (2005) Effect of CO₂ supply and demand on zinc uptake and growth limitation in a coastal diatom. *Limnol Oceanogr* 50: 1181–1192
- Sunda WG, Price NM, Morel FMM (2005) Chapter 4: Trace metal ion buffers and their use in culture studies. In: Anderson R (ed) *Algal Culturing Techniques*, Elsevier Academic Press, Burlington MA, pp 52–55
- Szabo E, Colman B (2007) Isolation and characterization of carbonic anhydrases from the marine diatom *Phaeodactylum tricornutum*. *Physiol Plant* 129: 484–492
- Tortell PD (2000) Evolutionary and ecological perspectives on carbon acquisition in phytoplankton. *Limnol Oceanogr* 45: 744–750
- Yee D, Morel FMM (1996) *In vivo* substitution of zinc by cobalt in carbonic anhydrase of a marine diatom. *Limnol Oceanogr* 41: 573–577